Preliminary Design of a Laboratory Cylindrical Hall-Effect Thruster

A Senior Project

presented to

The Faculty of the Aerospace Engineering Department

California Polytechnic State University, San Luis Obispo

In Partial Fulfillment

Of the Requirements for the Degree

Bachelor of Science in Aerospace Engineering

By Scott McGrail and Sam Parker

June, 2012

Preliminary Design of a Laboratory Cylindrical Hall-Effect Thruster

Scott McGrail[1] and Sam Parker[2]
California Polytechnic State University, San Luis Obispo, CA, 93405

A 3-cm cylindrical Hall thruster with permanent magnets was designed and modeled. The goal was to design a Hall thruster for Cal Poly's propulsion laboratory of similar size and performance as Cal Poly's MiXI thruster. The design process began with an investigation into the physics of Hall thrusters and selection of certain thruster parameters. The selected parameters were the diameter and depth of the channel, the total power input to the system, the discharge supply voltage, the cathode voltage, and the propellant flow rates to the anode and cathode. These parameters were used to determine the operational characteristics of the thruster which were then used to complete the thruster's mechanical design. The thrust was estimated to be between 3 and 14 mN, the Isp was estimated to be between 900 s and 2100 s, and the efficiency was estimated to be between 33.3% and 75%.

Nomenclature

B	=	magnetic field strength [Tesla]
B_z	=	magnetic field strength along the z-axis [Tesla]
dA	=	derivative with respect to the area of the thruster channel [meters^2]
dz	=	derivative with respect to position on the z-axis [meters]
E	=	electric field strength [Volts/meter]
E_r	=	electric field strength along the radial direction [Volts/meter]
I_d	=	current from the discharge voltage supply [Amps]
I_H	=	Hall current [Amps]
I_i	=	ion beam current [Amps]
I_k	=	current from the cathode keeper voltage supply [Amps]
I_{sp}	=	specific impulse [seconds]
J_H	=	Hall current density [Amps/meter^2]
L	=	characteristic length of the plasma channel [meters]
$\dot{m}_a$	=	mass flow rate of the propellant to the anode [kilograms/second]
$\dot{m}_c$	=	mass flow rate of the propellant to the cathode [kilograms/second]
$\dot{m}_p$	=	mass flow rate of the propellant [kilograms/second]
n_e	=	electron density [meter^{-3}]
P_d	=	power input of the discharge supply [Watts]
P_{in}	=	total power input to the system [Watts]
P_k	=	power input of the cathode keeper supply [Watts]
P_T	=	total power input to the system [Watts]
r_e	=	electron Larmor radius [meters]
r_i	=	ion Larmor radius [meters]
T	=	thrust [Newtons]
V	=	voltage [Volts]
V_c	=	potential at the cathode of the thruster [Volts]
V_d	=	discharge voltage supply [Volts]
V_h	=	cathode heater voltage supply [Volts]
V_k	=	cathode keeper voltage supply [Volts]
v_e	=	electron velocity [meters/second]

[1] Student, Aerospace Engineering Department, smcgrail@calpoly.edu.
[2] Student, Aerospace Engineering Department, sparke03@calpoly.edu, AIAA Member.

w	=	width of the plasma [meters]
η_c	=	cathode efficiency [unitless]
η_o	=	electrical utilization efficiency [unitless]
η_T	=	total efficiency [unitless]

Constants

e	=	electron charge	$1.602176487 \times 10^{-19}$ C
g	=	gravitational acceleration	9.81 m/s^2
M	=	Xenon particle mass	$2.1960351298052 \times 10^{-25}$ kg
m	=	electron mass	$9.1093822 \times 10^{-31}$ kg

I. Introduction

SPACE based electric propulsion includes any system that uses electrical power to accelerate the reaction-mass and generate thrust. Electric propulsion (EP) provides many advantages over the more traditional chemical propulsion, primarily high efficiency. Therefore less propellant is required to change the velocity of the spacecraft using EP. This is possible because, unlike chemical propulsion, electric propulsion is not limited by the chemical energy of the propellant. Theoretically, thrust generated by electric propulsion systems is only limited by the amount of power that can be supplied [1] [2].

Several types of electric propulsion thrusters exist, but the two most popular for flight applications are gridded ion and Hall-effect thrusters. Gridded ion thrusters inject propellant through a cathode, where it is ionized, before being fed into a plasma chamber [3]. A series of grids at the exit of the chamber are electrically biased by a power supply; the potential difference between these grids acts to electrostatically draw ions from the plasma and accelerate them out the exit of the thruster. Once the ions have exited the thruster, a second cathode neutralizes the charged particles, preventing them from repelling each other away from the thrust direction.

A Hall thruster operates on a similar principle of electrostatically drawing ions from plasma and accelerating them. Instead of electrically charging grids, however, an induced magnetic field captures electrons that emanate from the hollow cathode. In Hall thrusters, electrons exit the external cathode and are attracted to the positively charged anode in the base of the plasma chamber. Before reaching the anode, the electrons encounter a perpendicular magnetic field, causing them to be deflected sideways; this phenomenon is described as *the Hall Effect* [4]. The electrons then rotate radially about the center of the chamber; the resulting electric field electrostatically accelerates ions out of the thruster [3].

Hall thrusters have several advantages and drawbacks over their gridded ion counterparts [3]. Hall thrusters are mechanically simpler than gridded ion thrusters; they produce higher thrust, require less hollow cathodes, and require fewer power supplies for operation. Although they are mechanically simpler, the physics of Hall thrusters is more complex and involved than for ion thrusters. Also, Hall thrusters generally achieve slightly less electric efficiency and specific impulse than ion thrusters.

This report discusses the design of a small, cylindrical laboratory stationary plasma thruster (SPT). The thruster was designed to be operated in California Polytechnic State University- San Luis Obispo's propulsion laboratory. The objective of the project was to design a thruster of comparable size, efficiency, and thrust of Cal Poly's existing Miniature Xenon Ion thruster (MiXI).

II. Project Scope

When working with a system as complex as a Hall thruster, there are many different areas in which one could look for optimization or focus. One area of interest currently is scaling down Hall thrusters in both geometry and power for smaller satellite operations. Miniaturizing a typical annular Hall thruster however, introduces many new complications with regard to heating small elements in the thruster channel. For this reason, a new type of Hall thruster called a Cylindrical Hall thruster (CHT) was developed. These CHTs provide a smaller surface-to-volume ratio when compared with conventional annular Hall thrusters, therefore reducing undesired effects in the thruster like sputtering. This low ratio also allows for the scaling down in geometry and power desired for these small satellite operations [5].

This project combines elements of other small CHTs produced at MIT and Princeton in order to produce a complete working design. The design includes magnetic field strength and configuration, power input, thruster geometry, and predicted performance for this thruster. This project does not include the search for optimal design parameters; it instead focuses solely on producing a theoretically working CHT with reasonable parameters. In addition, this report will detail a suggested physical design and magnet configuration for students who might want to

build and test this particular thruster in a future project. The main goal of this project is to gain a fundamental understanding of the physical and mechanical operation of a Hall thruster, both theoretically and experimentally.

III. Hall Thruster Operation

In a Hall thruster, the propellant is split between the anode and the hollow cathode. The hollow cathode operates to create a negatively charged plasma cloud outside the thruster channel. Electrons leaving the cathode split; some are attracted to the positively charged anode inside the base of the thruster's channel, while the other electrons combine with the positively charged Xenon ions to neutralize the ion beam at the thruster's exterior. The radial magnetic field, travelling from the center stem out to the thruster wall, prevents the electrons from streaming straight to the anode and collecting. Instead, these electrons become trapped and spiral along the magnetic field lines in the *ExB* azimuthal direction around the channel, diffusing by collision into the anode and walls. Neutral propellant is pumped into the base region of the channel near the anode. These neutral propellant atoms collide with the electrons trapped in the channel and the propellant ionizes. The now free Xenon ions are accelerated across the electric field made between the anode and the negative potential outside the thruster created by the hollow cathode. This acceleration of the ions creates the thrust beam. The azimuthal drift of the electrons inside the thruster channel is known as the Hall current, giving the thruster its name [3]. These principles are demonstrated in Figure 1.

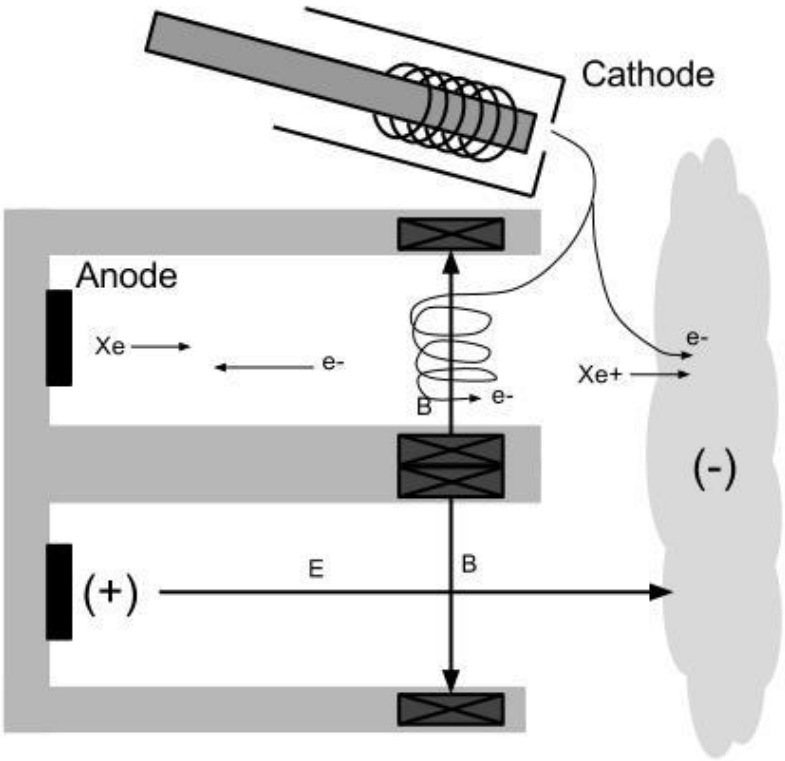

Figure 1. This is the conventional setup for an annular hall thruster.

Unlike conventional Hall thrusters, cylindrical hall thrusters do not have the center stem that provides the radial magnetic field. Instead, the channel becomes a chamber, as shown in Figure 2. There might be a small annular part, but this usually does not extend far into the thruster. The reason for removing the center stem is due mainly to heating and space. CHT's are typically much smaller than conventional hall thrusters, therefore scaling down the center stem would cause it to essentially become a small rod protruding through the center of the thruster, too small to house magnets, and it would heat up extremely quickly, past the critical temperature of the material. To mitigate this heating, the center stem is removed, so a different magnet configuration must be designed to produce the same effects. The design shown in Figure 2 is a standard CHT configuration.

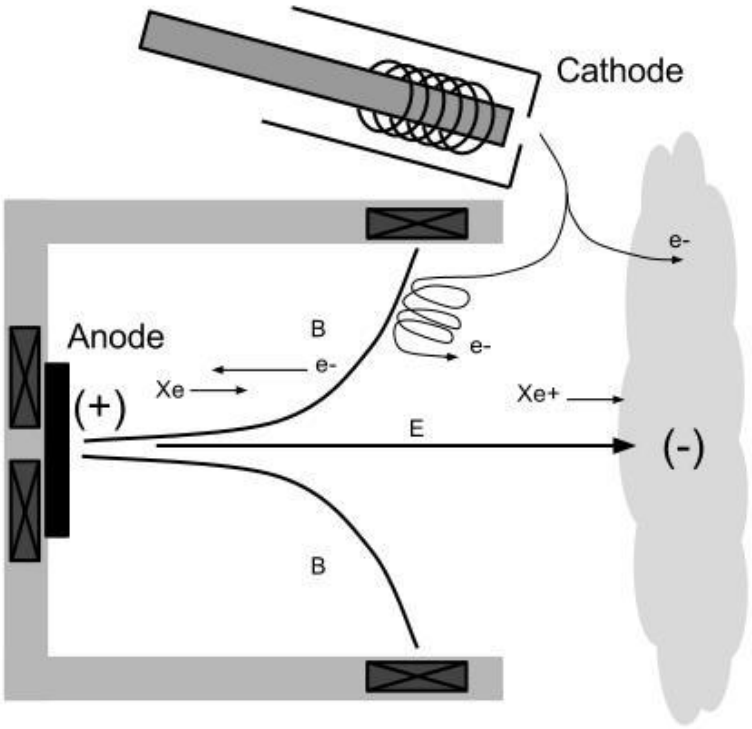

Figure 2. This shows the setup for a miniature cylindrical hall thruster.

With this configuration, the direct radial magnetic field is lost; therefore the thrust production is slightly different. The radial component of the magnetic field crossed with the azimuthal electron current produces thrust in this configuration. Also, the principals involved in trapping the plasma are slightly different than in the annular Hall thruster. An effect called magnetic mirroring keeps the plasma trapped so that the neutral propellant atoms can ionize. As the plasma particles travel toward the anode, they bounce off of the high magnetic field strength, shown where the magnetic field lines pinch together in Figure 2. The term "mirror" comes into play because the plasma particles are reflected back toward the negative potential outside the thruster by the strong magnetic field. Essential to the neutral propellant ionization, these electrons are trapped between the magnetic mirror and the negative potential at the thruster chamber exterior.

IV. Constraints and Considerations

Several internal and external constraints influence the scope and direction of this project. Due to previous work at Cal Poly with the Miniature Xenon Ion thruster (MiXI), it would be beneficial for future students if a Hall thruster of similar size were designed in this project. This could lead to comparisons in thrust, efficiency, and other performance parameters that could provide students an understanding of the fundamental differences between gridded ion thrusters like MiXI and Hall thrusters. For this reason, the chamber diameter is limited to about 30 millimeters, the same as MiXI's.

This Hall thruster is also designed with testing operations in mind. If the thruster is built and operated in the future, it must be compatible with the Aerospace Engineering Department's available vacuum chambers. With the current available equipment, this means limitations on propellant throughput and available power for the thruster to utilize. The total throughput of the thruster is limited to under 10 sccm to ensure proper operation in Cal Poly's vacuum chambers and that the current available flow control devices can handle the propellant.

As mentioned in the previous section, small CHTs are scaled down from larger conventional Hall thrusters in relation to the power supplied to the thruster. This means that a thruster of this class will probably be operated somewhere in the 50-200 Watt range, which will stand as a constraint for this project as well.

Finally, the design will be constrained to utilize permanent magnets rather than electromagnets, since this will reduce the power required for thruster operation and increase the overall and electrical efficiencies of the thruster.

V. Design Process

A. Considered Approaches

Several approaches allow for the determination and design of a Cylindrical Hall-Effect Thruster. One approach presented by Khayms and Martinez-Sanchez of MIT takes the operating parameters of a full-scale annual Hall thruster and scales them down based on laws that relate these parameters to changes in physical size [6]. This process aims to reduce the physical size and power requirements of an existing thruster while maintaining the thruster's specific impulse and efficiencies. Khayms and Martinez-Sanchez developed a series of equations that describe how the various densities, electron temperature, current density, and other parameters change with the size of the thruster. While successful in theory, this approach was a failure in practice; in operation, the scaled down thruster designed by Khayms and Martinez-Sanchez achieved much lower efficiency than had been predicted.

Another approach, first attempted in this project, was to develop the performance characteristics through a model of the plasma physics operating within the channel of the miniature thruster. While this is a completely valid approach, it is extremely difficult to understand and model the magnetohydrodynamics of operation.

Using this approach, parameters such as Hall current and current density are calculated in order to determine the performance of the thruster. The equation for Hall current is

$$I_H = n_e e\left(\int_0^L v_e dz\right)w = n_e e\left(\int_0^L \frac{E}{B} dz\right)w, \tag{1}$$

where *w* is the width of channel [3]. This can be approximated in 1D by the equation

$$I_H \approx n_e e w \frac{V_d}{B}, \tag{2}$$

however the number density of the electrons in the plasma must be determined to utilize this approach. [3] Using the quasineutral assumption, the electron density can be approximated by the plasma density, however finding the density of the plasma is also difficult to determine inside the thruster.

Thrust can then be found using

$$T = \int\left(\vec{J}_H \times \vec{B}\right)dA = I_H B \approx I_i \sqrt{\frac{MV_d}{2e}}, \tag{3}$$

yet again, another unknown enters the equation, the ion current [3]. If the plasma parameters were determined, solving these few equations would provide a simple way to determine thruster performance, yet determining these parameters is complicated, and therefore this approach will not be used in this report.

The final approach is to select design points and develop the performance from those specific input parameters. While this approach requires many assumptions, it provides an appropriate first-order analysis of the CHT's performance.

The three approaches outlined in this section were taken under consideration in the beginning stages of design, yet ultimately the third approach was chose as the appropriate method for a more detailed design in the scope of this project.

B. Assumptions

As mentioned previously, a fair number of assumptions must be made in order to utilize the design process. Many of these assumptions are required for the other approaches as well. Without a thorough understanding of magnetohydrodynamics or advanced plasma physics, the assumption that the plasma both inside and outside the thruster is quasineutral will be utilized. Quasineutrality allows uniform plasma densities and temperatures to be applied throughout the length and width of the plasma, while equating the electron density and the ion density, which simplifies the physics. Although this is not truly the case in a thruster, quasineutrality provides a decent starting point for analysis.

One of the main assumptions specific to the chosen approach is that the cathode efficiency is approximately equal to the total efficiency of the CHT. The cathode efficiency is the ratio of propellant routed to the hollow

cathode to the overall propellant delivered to the thruster. Plasma from the hollow cathode is "injected exterior to the discharge channel ionization region," so the propellant routed to this region is considered "lost," leading to the efficiency shown later in Eq. 12 [3].

Another important assumption in this approach is that the electron temperature inside the thruster ionization region is approximated as 1/10 of the beam voltage. Observations of Hall thrusters have led to this "rule of thumb." [3] Without a decent grasp of plasma physics, it would be difficult to determine the electron temperature inside the cylindrical chamber without making this assumption.

For this design, it will be assumed that the plasma region inside the thruster fills the entire chamber. This means that the characteristic length of the plasma is the same as the thruster length and the characteristic width is the size of the thruster diameter.

C. Physics Model Approach

The chosen approach requires that the designer "set" certain parameters of the CHT in order to carry out the analysis and determine the thruster performance. The inputs for this model are the physical dimensions of the thruster, i.e. the diameter and length of the chamber, the total power input to the system, the discharge supply voltage, the cathode voltage, and the propellant flow rates to the anode and cathode. With these inputs, the operational characteristics of the CHT can be determined as follows. Note that all analysis is done with magnitudes rather than vectors. This simplifies the model and allows for one to ignore the changing electric and magnetic fields throughout the thruster channel.

With the variance in the input power, P_{in}, comes a variance in the discharge supply, V_d. Also, the cathode voltage, V_c is really dependent upon the hollow cathode operation. The difference of these two potentials provides an approximate value for the beam voltage, V_b, since the beam spans from the anode to the cathode, as shown [3]

$$V_b = V_d - V_c. \tag{4}$$

This potential difference creates the electric field, E, essential to the thruster's operation using

$$E = \frac{V_d - V_c}{L}, \tag{5}$$

where L is the length of the thruster in meters, from anode to the negatively charged plasma just outside the thruster chamber [3].

With the electric field strength, the drift velocity of the electrons trapped inside the chamber can be determined. This is typically determined as a vector with the equation

$$\vec{v}_e = \frac{\vec{E} \times \vec{B}}{B^2}, \tag{6}$$

however with the analysis performed with magnitudes only, Eq. 3 can be approximated by

$$v_e = \frac{E_r}{B_z}, \tag{7}$$

where E_r is the electric field strength in the radial direction in volts per meter and B_z is the magnetic field strength in the radial direction from the centerline of the thruster in Tesla, yielding a azimuthal velocity in meters per second [3].

This electron velocity is integral when determining the Hall current in the thruster, which is one of the main parameters in determining the performance of the thruster. However, as mentioned previously, this physics approach will not be taken. This velocity can be used, however, to determine the Larmor radius of the electrons. It is important to find the Larmor radii of the ions and electrons in the plasma to ensure that the plasma is being sufficiently trapped in the chamber. The electrons need to provide the Hall current, otherwise there will be no thrust. This can be done by ensuring that the electron Larmor radius is much less than the characteristic length of the thruster, as shown by [3]

$$r_e = \frac{1}{B}\sqrt{\frac{2mv_e}{e}} = \frac{1}{B}\sqrt{\frac{8mT_e}{\pi e}} << L \quad , \tag{8}$$

where m is the mass of an electron and e is the charge of an electron.

Due to the variation in the electric and magnetic fields inside the thruster, it is difficult to know if the calculated electron drift velocity from Eq. 7 provides a valid parameter. It is easier to use the second form of the equation because of the assumption made for this approach, which says that [3]

$$T_e \approx 0.1V_b \quad . \tag{9}$$

Making this substitution in Eq. 8 allows the determination of the electron Larmor radius.

When determining the ion Larmor radius, it is important to remember the purpose of the ions in the Hall thruster. The ions collect in the beam and are accelerated out of the thruster through the electric field. If the magnetic field is too large, these ions would be trapped in the chamber of the thruster and no thrust would be produced. For this reason, the ion Larmor radius, calculated as shown, should be much greater than the length of the channel [3],

$$r_i = \frac{1}{B}\sqrt{\frac{2MV_b}{e}} >> L \, . \tag{10}$$

where M is the mass of a Xenon particle, and e is the charge of a single electron.

Another reason for using the second form of the electron Larmor radius equation is for use in determining the magnetic field strength required for thruster operation. Both Eq. 8 and Eq. 10 utilize the same inputs, namely B and V_b, and therefore can be iterated in order to determine an appropriate magnetic field strength for the operating parameters and physical characteristics of the thruster.

Now that the magnetic field strength has been determined, it is important to start looking at the overall performance of the thruster. This is where the assumption on efficiency will be utilized. The mass flow rates of the propellant delivered to both the anode and the cathode are defined by the user. The total propellant mass flow rate is [3]

$$\dot{m}_p = \dot{m}_a + \dot{m}_c \, . \tag{11}$$

Using this definition, the cathode efficiency can be found by [3]

$$\eta_c = \frac{\dot{m}_c}{\dot{m}_p} \, . \tag{12}$$

The assumption stated earlier allows [7]

$$\eta_T \approx \eta_c \, . \tag{13}$$

Using thrust production, the total efficiency can be calculated with [3]

$$\eta_T = \frac{T^2}{2\dot{m}_p P_{in}} \quad . \tag{14}$$

Since propellant flow rate, efficiency, and input power are all known, Eq. 14 can be rearranged to solve for thrust using [3]

$$T = \sqrt{2\eta_T \dot{m}_p P_{in}} \,. \tag{15}$$

With thrust now known, performance in the form of specific impulse can be calculated with the standard equation [3]

$$I_{sp} = \frac{T}{\dot{m}_p g} \,. \tag{16}$$

D. Parts and Hardware

After investigating the physics of Hall thrusters and determining some of the operating parameters, the thruster itself was designed. This was a challenging process; the thruster went through much iteration before a mechanical design was converged upon. Simplicity, manufacturability, durability, and cost were some of the main considerations when mechanically designing the thruster. This section discusses the mechanical design process of the CHT, as well as some of the components that will be needed for operation.

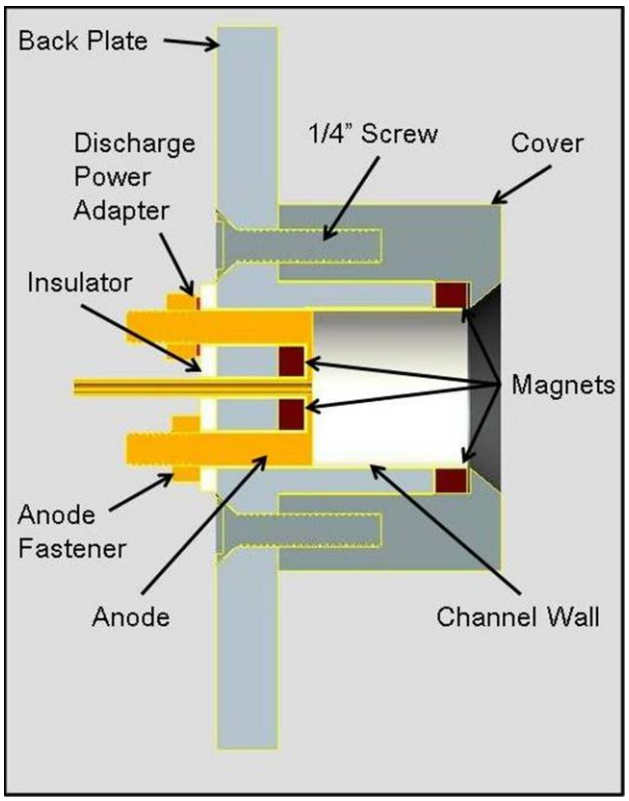

Figure 3. This is a cross sectional view of the solid model of the CHT.

Figures 3, 4, and 6 show the model of the current thruster design. Figure 3 shows a cross sectional view of the solid model. Figure 4 is an exploded view of the thruster design will all of the components labeled. The current configuration of the CHT consists of many separate parts that are press fit together. There are a total of 20 permanent magnets and 12 different parts that make up the system (not including the six screws that fasten the cover to the back plate). In addition to the magnets, there is an anode, a channel wall, a backing plate to hold the components together and attach the thruster to a test stand, and five individual pieces that make up the anode insulator. A steel cover is placed over the top of the other components and screwed into the backing plate to hold everything together. An attachment to the discharge power will rest on one of the posts of the anode, and two fasteners will secure the anode to the back plate.

While designing mechanical configuration of the thruster, the main goal was to create the environment that would allow the thruster to meet its design criteria. In order to accomplish this goal, many factors had to be

considered; primarily, the material temperature ranges, magnet placement, anode isolation, and manufacturing limits. Also, a lot of thought went into how the thruster components would be brought together. Eventually, a press fit system was developed; this allowed the primary functional components to be sandwiched between a backing plate and a cover plate, which are screwed together.

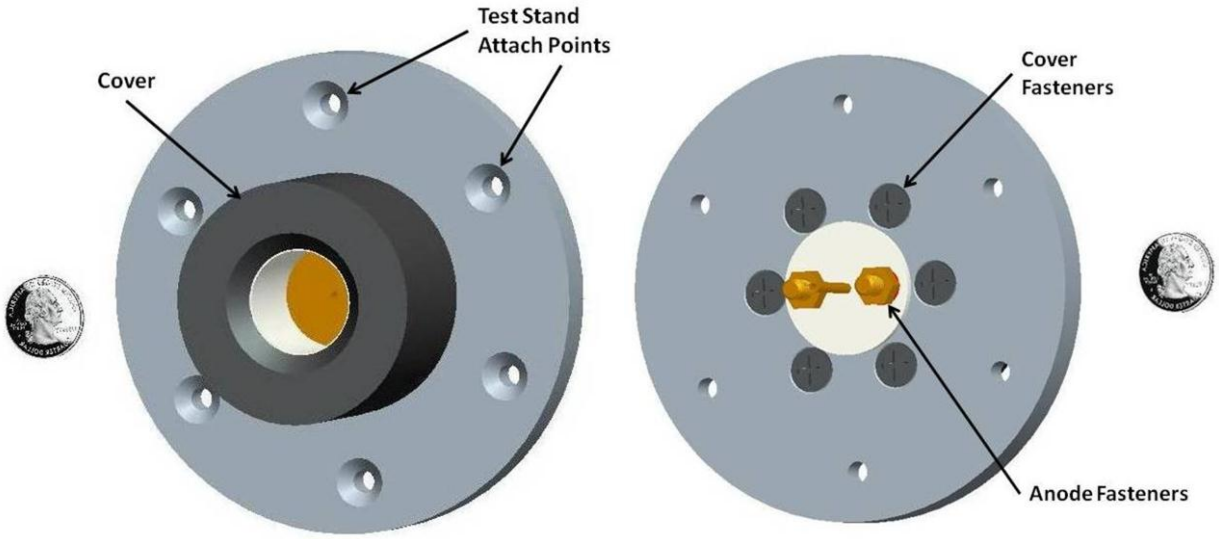

Figure 4. This shows the front and back of the CHT compared to a US quarter.

At the heart of the thruster assembly is the anode. The anode's purpose is to draw electrons emanating from the hollow cathode into the channel. In order to draw electrons into the channel, the anode must have a potential bias and therefore must be made from a conductive material. The anode is the most complicated piece of the assembly and it must be manufactured with precision. Due to the small size of the thruster and the high tolerances on the dimensions, the material must also be easy to machine. Also, to reduce the chance of the anode or insulators cracking due to thermal expansion, the material must have a very low thermal expansion coefficient.

When selecting the material for the anode, melting temperature, thermal expansion coefficient, dollars per kilogram, and manufacturability were considered. The variety of viable materials was narrowed down by researching historical Hall thruster designs and limiting the choices to the most commonly used materials. The materials considered were: molybdenum, tantalum, tungsten, and stainless steel. The metals and their respective metric values are listed in Table 1. Since manufacturability is not a quantifiable metric, each material was ranked based on their relative ease to machine. No final decision was made as to what material should be used for the anode, but steel is clearly a poor choice because of its low melting temperature and thermal expansion coefficient. Molybdenum, tungsten, and tantalum are all viable options. Molybdenum is the recommended material because of its low cost and low thermal expansion coefficient; plus it is relatively easy to machine [6]. However, experimenting with anode materials is an option for a future project.

Table 1. Anode material properties [15] [16].

Material	Manufacturability (-)	Melting Point (^{o}C)	Thermal Expansion coefficient (μm/m ^{o}C)	Cost ($/kg) [May, 2011]
Molybdenum	2	2,623	4.8	37.70
Tungsten	4	3,422	4.5	40.80
Stainless Steel	1	1,450	12	0.56
Tantalum	3	3020	6.5	264.554

Figure 5 shows the solid model of the anode. The anode will make up the entire back wall of the channel. As in all Hall thrusters, the propellant will be fed into the channel through the anode. To accommodate this feature, the anode has a long tube that extends out the back of the thruster. At the end of this long tube, the propellant feed lines will be attached. It should be acknowledged that an interface between the anode and the propellant lines has not yet been designed. This interface will have to be designed before the thruster can be operated and must ensure that the anode is insulated from the propellant lines [8].

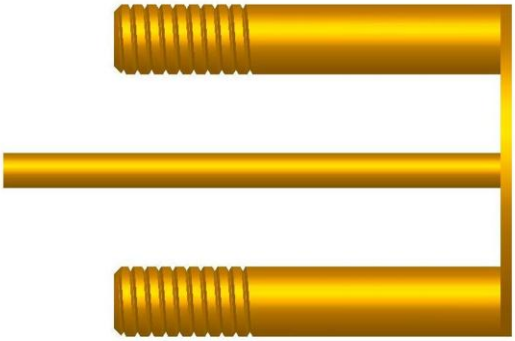

Figure 5. This is the solid model of the CHT's anode.

Another feature of the anode is the two additional solid posts extend out the back. These posts serve two purposes, the first one being to provide a place for the discharge power connector to be attached. This connector is what supplies the discharge power, which is what causes the positive potential in the anode [8] [6]. The second purpose for the posts is to allow the anode to be attached to the back plate. Two fasteners will be screwed onto these posts to secure the anode to the back plate, which will prevent the anode from slipping into the plasma channel. This is part of the press-fit design that will hold the assembly together.

The wall of the Hall thruster channel is also usually made of dielectric materials because of their minimal reactance with plasma. When selecting material for the channel wall, it is important to choose something that will have a low secondary electron yield; this quality is common among dielectric materials such as Boron Nitride and Alumina [3]. Like the anode, the wall material must be capable of withstanding very high temperatures and have a low thermal expansion coefficient [8] [6] [5]. There is a variety of materials that meet this criteria, and to narrow down the options, only the most commonly used on Hall thrusters were considered. The options were narrowed down to Alumina, and Boron Nitride. Table 2 shows the options along with some of the material properties that were weighed. No conclusion was made about which material should be selected, it is recommended that Boron Nitride be used, but alumina is the less expensive option and is capable of doing the job. As with the anode, experimentation is recommended to determine the more desirable channel wall material.

Table 2. Channel wall and anode insulating material properties [3] [15] [16].

Material	Manufacturability (-)	Melting Point (^{o}C)	Thermal Expansion coefficient (µm/m ^{o}C)	Secondary electron yield [at 40 eV]	Cost ($/kg) [May, 2011]
Alumina (Al_2O_3)	1	2,072	5.4	1.5	2.50
Boron Nitride (BN)	2	2,973	2.7	1.24	~128.00

In order to maintain a positive potential bias, the anode must be insulated from the rest of the assembly with a non-conductive material. These insulators, as well as the channel wall, are represented by the white components in Figs. 3, 4, and 6. In the design of this CHT, there are plans for five individual pieces that will provide insulation to the anode. One disk-shaped insulator will protect the back of the anode from coming into contact with the back plate. Three tube-shaped insulators will act as a barrier between the back plate and the posts and propellant feed portion of the anode. The final piece, another disk shaped object, will rest behind the back plate and prevent contact between the back plate and the fasteners. These insulators are very important and ensure that there is no short-circuit between the anode and any other conductive material. Because of the high melting temperature and low conductivity, the same material used to make the channel wall can be used to make the insulators.

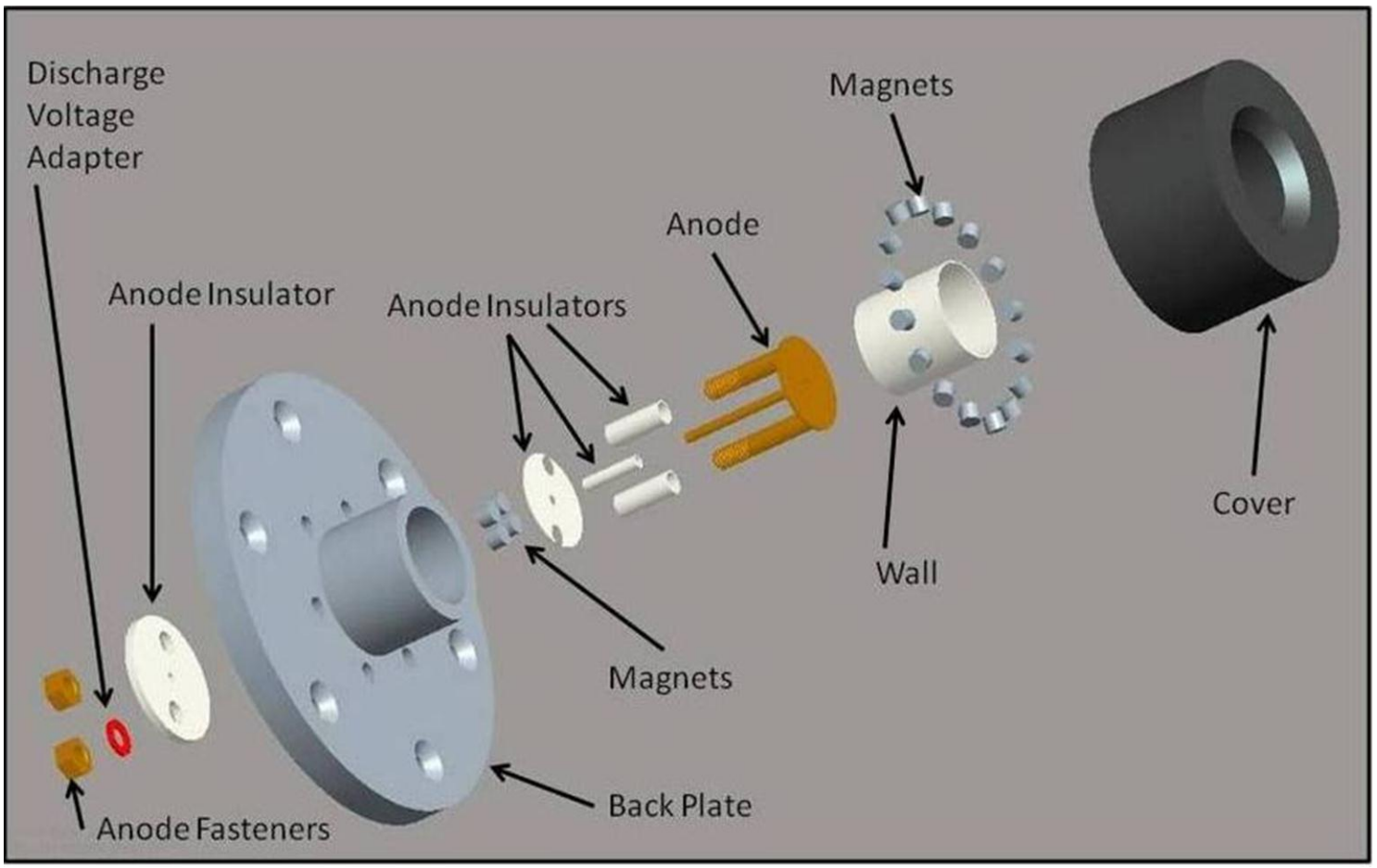

Figure 6. This is an exploded view of the solid model of the CHT. It is shown without the screws that fasten the back plate and cover together. Note that the back plate and cover are made of the same material, but are shown in different colors.

The geometry of the channel and the magnetic field strength were flowed down from the constraints and physics involved. The next step was to determine the size and quantity of permanent magnets required to achieve the desired magnetic field strength inside the channel. Since the magnetic field strength of permanent magnets depends on their size, shape, and material, a magnet had to be selected before any real analysis could begin. For the sake of simplicity and cost, only commercially available permanent magnets were considered.

Many magnet shapes and sizes were considered, but it was ultimately determined that disk magnets would be the most ideal for the purposes of this project. Disk magnets are very inexpensive and their shape allows simpler analysis of their magnetic field characteristics, making them well suited for this project [9]. The size of commercially available disk magnets can range from 0.1 inches in diameter to over two inches in diameter, and 0.06 inches in thickness to one inch in thickness. The appropriate magnet size was decided upon after several iterations of the mechanical design. The main issue was that magnetic inductance decreases with distance from the surface of the magnet; therefore it's important to find magnets that are large enough to provide the desired magnetic field strength but small enough to fit inside the thruster casing. It was ultimately determined that 0.25 inch diameter, 0.20 inch thick permanent magnets would be the most adequate commercially available size [10].

The other important parameter that needed to be determined was the permanent magnet's material. It was important to choose a material that could provide the strongest magnetic field away from the surface and withstand the high temperatures that are a byproduct of the plasma in the channel [5] [8]. In keeping with the requirement that only off-the-shelf permanent magnets be used, three common magnetic materials were considered: Neodymium iron boride (NdFeB), aluminum nickel cobalt (AlNiCo), and samarium cobalt (SmCo). The characteristics of each type of magnet also depend on the magnet's grade; the grade is typically the maximum energy product ($BH_{max)}$ of the material in mega Gauss-Oersted [9]. Table 3 lists some characteristics of various magnet materials and material grades.

Table 3. Properties of various magnetic materials and material grades [11] [10].

Material and Grade	BH_{max} (MGOe)	Br (kG)	Hc (kOe)	Max Working Temp. (^oC)	Curie Temp. (^oC)
NdFeB N35	35.0	12.10	11.40	80	310
NdFeB N42	42.0	13.30	12.30	80	310
SmCo 18	18.0	8.50	8.00	260	750
SmCo 26	26.0	10.50	9.20	350	825
AlNiCo 8	5.3	8.20	1.65	540	890

Several characteristics were looked at when selecting the magnetic material and grade. Residual flux density (Br) is the magnetization that remains in a magnetic material after an external magnetic field has been removed [9]. The coercive force (Hc) is the demagnetizing force that is required to reduce the magnetization from saturation to zero [9]. The maximum working temperature is the temperature at which a permanent magnet will begin to lose strength [9]. The Curie temperature is the temperature at which the permanent magnet becomes demagnetized [9].

The maximum working temperature and Curie temperature were of particular importance due the high temperatures in and around the thruster during operation. The low working temperature of Neodymium magnets eliminated them from contention. While Alnico magnets have very high working temperatures, their maximum energy product is far too low. The best compromise between high working temperature and high maximum energy product turned out to be samarium cobalt, grade 26 [10].

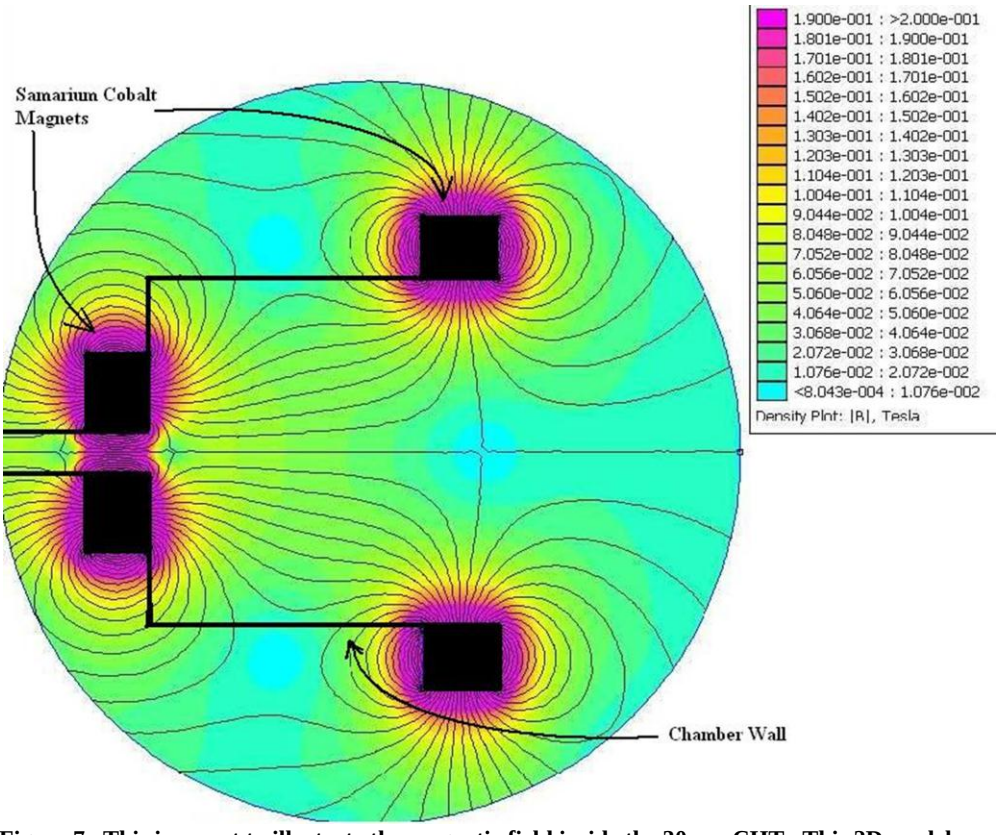

Figure 7. This is meant to illustrate the magnetic field inside the 30mm CHT. This 2D model was generated using Finite Element Method Magnetics and used four SmCo-26 magnets. The model assumed no attenuation due to the chamber wall [11].

After selecting the size and type of magnet, some simple analyses were conducted to determine the magnetic field strength should be expected inside the channel. This was accomplished using the software tool 'Finite Element Method Magnetics' or FEMM. FEMM is an open source analysis tool that performs finite element analysis on permanent magnets as well as electromagnets. It was created by Dr. David Meeker and is an accurate model of

magnetostatic field interactions. FEMM works under the assumption that the field is time-invariant and the magnetic material is linear isotropic; it then applies these assumptions to Maxwell's equations to model the magnetic field [11].

Figure 7 shows the two-dimensional cross-section of the magnetic field that was generated using FEMM. It should be noted that this is a simplified model that assumed the walls of the chamber had no attenuating affects on the magnetic field strength; air is the only thing assumed to be separating the magnets from one another. This means that the only thing affecting the magnetic field of this model is the magnet type and position relative to the other magnets. The four black squares in the figure are the samarium cobalt-26 magnets, and the thick black lines represent the channel wall of the thruster. The magnets were positioned on the outside of the channel wall close to the exit of the thruster and behind the back channel wall. This is a common configuration for CHTs and allows the magnetic field to capture electrons in the plasma chamber before they reach the anode [12]. The magnetic field in Figure 7 indicates that the field strength at the surface of the magnets will be in excess of 2,000 Gauss, but drops significantly distance from the surface. According to Figure 7, the magnetic strength can drop to as low as 80 Gauss inside the thruster channel. However, the 800 Gauss region is roughly where it needs to be, in the center of the channel, about halfway between the magnets at the exit and at the inlet.

To support all of these components, a main thruster body is needed. This part of the assembly consists of the backing plate, which is the component that most of the parts attach to, and a cover. These parts are shown in the exploded view of the assembly in Figure 6. They can also be seen in Figure 4, where they are shown juxtaposed to a US quarter-dollar to demonstrate the thruster's relative size. In the models, the backing plate and the cover are shown as different colors to distinguish them as individual components. Most of the components will rest inside, or be attached to the backing plate; the cover holds the channel wall and the magnets in place and is fastened to the backing plate via six screws. Because they do not contribute to thruster performance, no analysis was done to determine the best size or material for these components. It was decided that stainless steel would be an ideal material due to its high melting temperature and inexpensive cost.

In order to run the CHT, there is a lot of circuitry that must be set up. Three main power supplies are required for this type of Hall thruster with permanent magnets. The main supply is the discharge supply, V_d. This connects directly to the anode in the thruster and provides the positive potential at base of the thruster's chamber [3]. The other two supplies are connected to the hollow cathode for operation. The heater supply, V_h, is used once the chamber is pulling significant vacuum, and is used to heat up the hollow cathode before propellant is allowed to flow through it. If not sufficiently heated or under vacuum, the propellant running through the cathode will poison the cathode, rendering it unusable [3]. Once the cathode is sufficiently heated, the propellant can begin to flow and the cathode should supply plasma to the thruster. If this process is successful, the cathode will be almost self-heating, and the heater supply can be shut down. To supplement the heating from the plasma in the hollow cathode, the keeper supply, V_k, at a much lower voltage than the heater supply, will be turned on [3]. The electrical schematic for this can be seen in Figure 8.

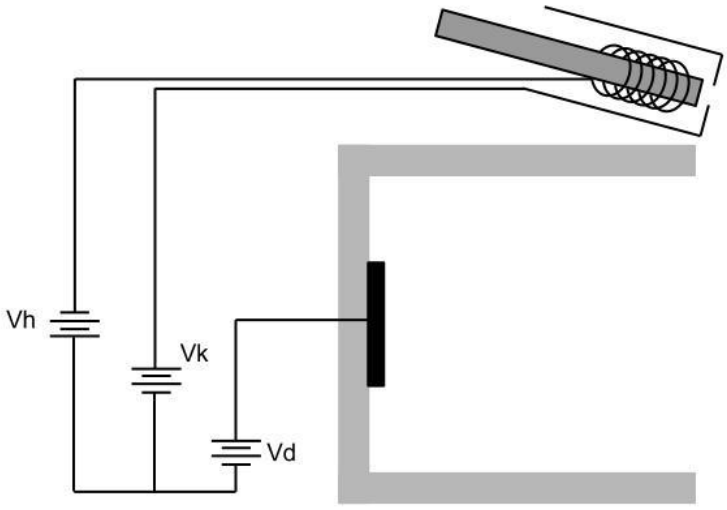

Figure 8. This shows the electrical setup for the CHT.

VI. Expected Performance

Using the described physics model in section IV-C, the expected performance and parameters of the CHT can be found. Before the parameters like thrust, Isp, and efficiency can be determined, the input parameters must first be stated. Due to the size and constraints of this design, the CHT will be a lower power thruster. For this reason, the total input power is constrained to between 50 and 200 W. Along with this input power, the discharge voltage supply, V_d, will be between 50 and 100 V. The potential of the plasma cloud output by the hollow cathode is assumed to be approximately 12 V [13]. This could be measured experimentally and is dependent upon the hollow cathode used in the experiment. These input values provide a range of electric field strengths, between 1266.7 and 2933.3 V/m, from the base to the exit of the chamber.

The magnetic field strength at the centerline of the thruster helps determine the Larmor radii of the ions and electrons. These radii can vary, as long as the electron Larmor radius is much smaller than the characteristic length, and the ion Larmor radius is much greater than this length. To determine an acceptable magnetic field strength, several strengths were tried to see the outcome of the Larmor radii based on the discharge voltage. Figure 9 was generated with a magnetic field strength of 800 Gauss at the centerline of the thruster.

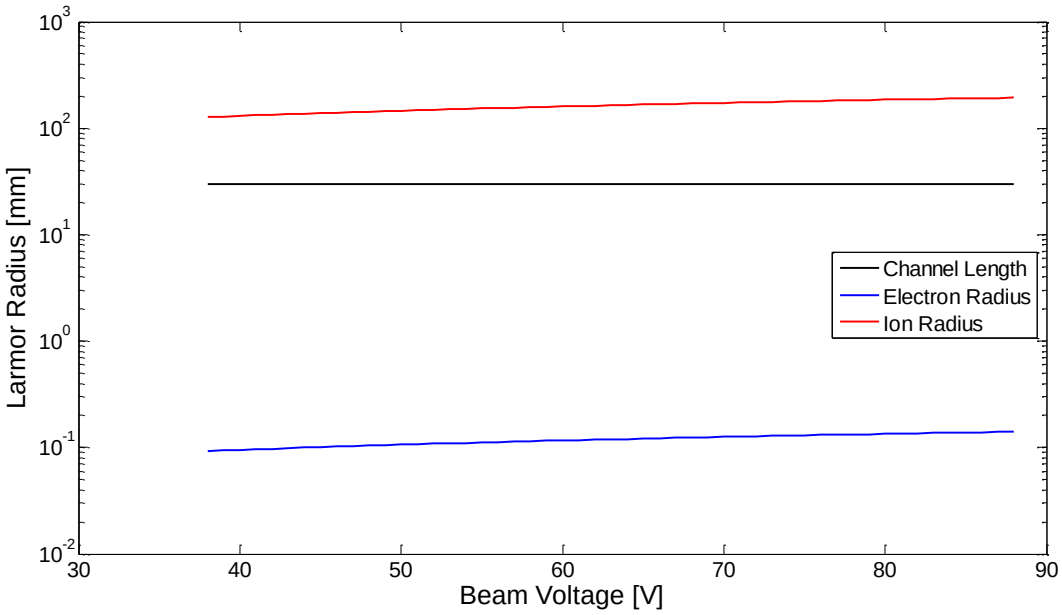

Figure 9. This figure shows the Larmor radius for both the ions and the electrons at 800 Gauss magnetic field strength across the distribution of discharge voltages.

As the orders of magnitude on the y-axis show, both the Larmor radii are appropriately scaled with respect to the length of the channel, represented by the black line on the figure. While 800 Gauss is an acceptable strength for the magnetic field, it is not the optimal magnetic field strength; however, since the goals of this project do not include finding an optimal design, 800 Gauss will be used as the design point for the magnetic field in the chamber of the CHT. As stated earlier, the approximation for electron temperature in the electron Larmor radius equation through a fraction of the beam voltage is used, simplifying the plasma physics involved in the model.

The remainder of the analysis will be conducted using a constant mass flow rate of 2 sccm of Xenon to the cathode. Keeping the cathode flow rate constant allows the variance of the anode mass flow rate and the overall performance trends to be calculated. As mentioned, one of the larger assumptions made in this analysis allows the total efficiency to be approximated by the cathode efficiency, as shown in Eq. 13. The authors of this report believe this is a valid assumption to make, however further work on this project would allow the validation of the assumption. With a constant cathode mass flow rate, the efficiency of the thruster changes only based on the mass flow rate to the anode. These anode flow rates are varied from 1 to 6 sccm Xenon for the analysis. Using Eq. 12 and the stated mass flow rates of propellant, the total efficiencies of the thruster for the analysis are 33.3%, 50%, 60%, 66.7%, 71.4%, and 75% efficient. This range, from mid-thirties to eighty percent efficient, encompasses typical efficiencies of smaller electric propulsion thrusters [13]

Solving Eq. 15 with the total propellant flow rates, efficiencies, and the specified range of input power, the predicted thrust output of the CHT can be found.

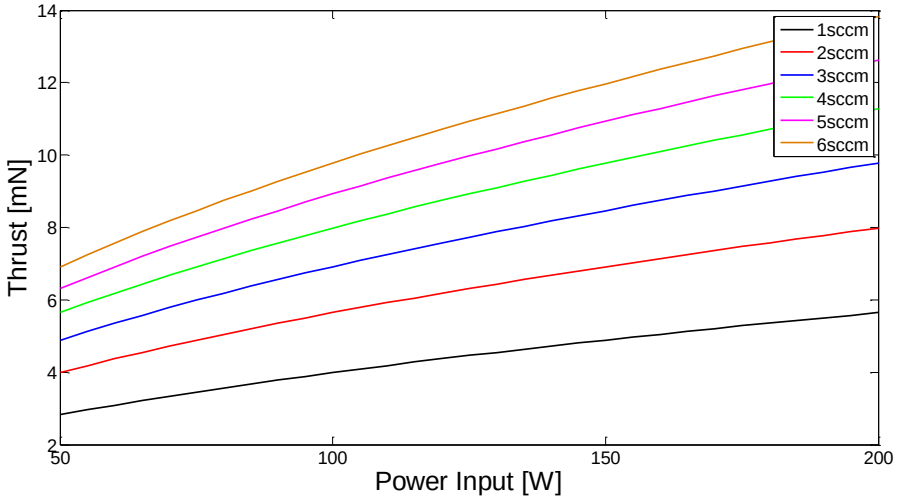

Figure 10. This figure provides the output thrust of the CHT for different anode propellant flow rates, while keeping the cathode flow rate constant at 2 sccm.

As shown in Figure 10, the thrust output of the CHT increases with both propellant flow rate to the anode and the power input to the system. One must be aware that this is a very simplified model of the workings of the CHT; running this CHT in future work at these flow rates could help validate the model. The thrust output, ranging from approximately 3-14 mN, is a fairly decent range of expected thrust values for a CHT of this size, if not a bit high. Since this model ignores many inefficiencies, like losses to the wall, higher thrust values can be expected from this first-order analysis.

Finally, relating thrust and the total propellant mass flow rate to the thruster through Eq. 16 yields values for specific impulse of the CHT. Unlike the thrust curves, the specific impulse curves decrease as the total propellant flow rate increases due to the inverse relationship. The resulting specific impulses can be seen in the figure below.

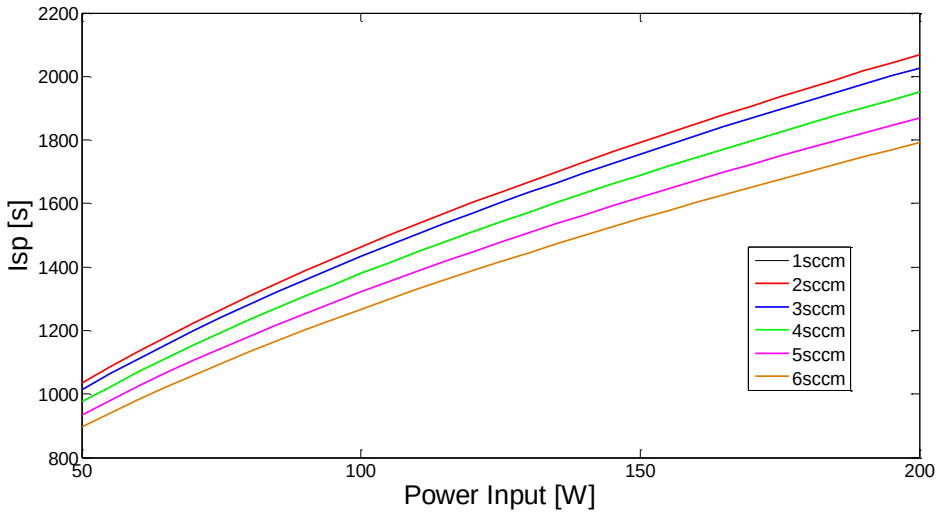

Figure 11. This figure shows the specific impulse of the thruster at each of the respective flow rates and thrust levels from Figure 10.

VII. Thruster Design Validation

When this thruster is built, it will be necessary to determine the performance of the thruster through measurements. The equipment required for this will include a thruster stand with a load cell to directly measure

thrust and a plasma diagnostic probe to place in the plume, capable of determining the electron density, electron temperature, and plasma potential. With these measured values, the actual performance of the thruster and the validity of the model in this report can be determined.

Placing the probe near the thruster exit, the plasma potential at this location, V_c, can be determined. This measured value can be used in Eq. 4 and Eq. 5 to determine the experimental beam voltage and electric field strength [13]. In turn, the beam voltage can then be used in Eq. 10 for the actual ion Larmor radius determination. The electron temperature can also be measured with the probe, and therefore used in Eq. 8 for determination of the actual electron Larmor radius.

The voltage and current displayed on the discharge and cathode keeper power supplies can provide the necessary information to determine the total power into the system, with permanent magnets, which is [3]

$$P_T = P_{in} = P_d + P_k = V_d I_d + V_k I_k . \tag{17}$$

With permanent magnets, this total power is smaller since there are no electromagnets, which would require another supply.

The electrical utilization efficiency can be calculated using [3]

$$\eta_o = \frac{P_d}{P_T} . \tag{18}$$

Utilizing Eq. 12 and Eq. 18, the actual total efficiency of the thruster can be determined with [3]

$$\eta_T = \frac{1}{2}\frac{T^2}{\dot{m}_a P_d}\eta_c \eta_o . \tag{19}$$

Solving this equation with measured parameters and the efficiencies calculated will either validate or discredit the assumption made for the physics model used, shown in Eq. 13.

VIII. Conclusion and Recommendations

Hall thrusters, especially miniature thrusters, have promising potential for the future of spacecraft propulsion. They can be utilized in several continuous burn applications like transfer trajectories, counteracting orbital perturbations, and high precision formation maneuvering. Smaller Hall thrusters require a design different than the conventional annular design, thus the CHT becomes a viable option to fill the need [14].

This project included a performance model of the thruster, a magnetic field analysis in the thruster chamber, and a solid model of the thruster's physical design. Theoretical design of a Hall thruster requires a thorough understanding of plasma physics and magnetohydrodynamics. This project was an exercise in learning about a subject that both authors had very little preceding knowledge about, attaining an understanding of the fundamental principles of its operation, and applying those principles to formulate a preliminary design. Many parameters must be assumed when designing a theoretical thruster, since several of these are measured quantities that are difficult to define theoretically. By utilizing the approach detailed in this report, the authors were able to develop a preliminary performance model for CHT.

Limiting the CHT to operate in the 50-200 W range keeps the thrust in a reasonable range for its size. With code written in MATLAB, the performance of the thruster was determined to range from 3 to 14 mN of thrust with specific impulse capabilities between 900 and 2100 seconds. Due to the simplification of the model used however, the major assumptions made must be validated empirically in the future through the fabrication and operation of this CHT.

Using Pro/Engineer and Finite Element Method Magnetics, a physical model of the thruster and magnetic field configuration inside the thruster chamber were designed. The final design of the CHT consists of 20 permanent magnets and 12 miscellaneous components. A press fit system will hold the components together by sandwiching them between a steel plate and a steel cover. An anode, a channel wall, and a layer of insulation were designed but the materials they will be made from are still to be determined. Material properties were investigated, options were narrowed down, and recommendations were made but the final material selection will be left to those who build the thruster.

The authors selected grade 26 Samarium Cobalt magnets with a diameter of 0.25 inches and a thickness of 0.2 inches. FEMM was used to make a simple, two-dimensional model of the magnetic field interaction of the thruster's magnets. The model indicated that the magnet's strength decreases greatly with distance, and the magnetic field strength in the channel will not be the constant 800 Gauss that was assumed in the preliminary calculations. Further analysis on the magnetic field should be conducted prior to construction of the thruster to determine whether the field strength will be sufficient enough to trap the electrons emanating from the cathode.

There are a few areas of future design and analysis that should be completed before the thruster is built. One area is a more thorough investigation into the magnetic interactions. The goal of this investigation is to determine what how the variations in magnetic field inside the channel might affect thruster performance While FEMM is a good first-order analytical tool, a three dimensional model of the magnetic field could provide a more accurate estimate of the magnetic inductance inside the channel.

The authors did not conduct any thermal analysis when designing the thruster. Thermal analysis is important because temperatures inside hall thrusters can rise to over one-thousand degrees Celsius [8]. Before building the thruster, the maximum expected operating temperature for each component should be estimated to confirm that the materials will withstand the extreme heat. In addition, a method for measuring the temperature of the magnets during thruster operation needs to be determined. The magnets should have the lowest melting temperature of any component of the thruster and it is important to ensure that their maximum working temperature is not exceeded. During operation, magnet temperature will have to be monitored and the thruster shut down when the working temperature is reached [13].

Also, it might be necessary to place some sort of shunt on the anode to decelerate the propellant as it enters the channel. The current design directly injects the propellant into the channel and there is some concern that it might spend too little time in the channel to be ionized. There needs to be assurance that the propellant is traveling slowly enough to be ionized before it exits the channel [8]. There also needs to an interface between the propellant lines and the anode that insulates the anode from the metallic propellant lines. Finally, before the thruster can be operated in the laboratory, a test stand needs to be built. Six holes around the outer part of the back plate provide a place to fasten the thruster to a testing apparatus; however, this apparatus has not yet been designed.

The ability to operate this CHT in the facilities available to the Aerospace Engineering Department at Cal Poly was a major factor in the design process. The authors of this report hope that students will build and operate this thruster to validate the model, or use this project to as a stepping-stone when building a higher fidelity model of a miniature CHT. There is also the hope that this thruster could provide future laboratory experiments and comparisons of Hall thrusters and a gridded ion thruster of the same size, like MiXI.

Appendix

Contact the authors of this report for Matlab code, Pro/E models, and FEMM models.

Acknowledgments

The authors of this report would like to sincerely thank Daniel J. Wait for his patience and guidance throughout the entirety of this project, Dr. Dan Goebel of JPL for his help and advice about wading through the many equations in his book, and David Knapp for his willingness to let us bother him every week for his electric propulsion and hollow cathode knowledge.

References

[1] G. P. Sutton and O. Biblarz, Rocket Propulsion Elements, New York: Wiley, 2010.

[2] R. G. Jahn, Physics of Electric Propulsion, Mineola, NY: Dover Publications, Inc., 1996.

[3] D. M. Goebel and I. Katz, Fundamentals of Electric Propulsion, Hoboken: Wiley, 2008.

[4] R. D. Knight, Physics for Scientists and Engineers, San Francisco, CA: Pearson Education, Inc., 2004.

[5] Y. Raitses, A. Smirnov and N. J. Fisch, "Cylindrical Hall Thrusters With Permanent Magnets," Princeton Plasma Physics Laboratory, Princeton, NJ, 2000.

[6] V. Khayms and M. Martinez-Sanchez, "Fifty-Watt Hall Thrusterfor Microsatellites," in *Mircorpropulsion for Small Spacecraft, Vol. 187, Progress in Aeronautics and Astronautics, AIAA*, Renton, VA, 2000.

[7] D. D. M. Goebel, Interviewee, *Email Exchange With Dan Goebel.* [Interview]. 4 April 2012.

[8] N. Z. Warner, "Theoretical and Experimental Investigation of Hall Thruster Miniaturization," Massachusetts Institute of Technology, Cambridge, MA, 2007.

[9] National Imports LLC-Magnetic Products, "Permanent Magnet Selection and Design Handbook," [Online]. Available: http://www.rare-earth-magnets.com/Permanent-Magnet-Selection-and-Design-Handbook.pdf. [Accessed 21 May 2012].

[10] "Magnetic Shop-Item # 26DRE1613, Small Samarium Cobalt Disk Magnets," Magnetic Shop, [Online]. Available: http://magnetsales.thomasnet.com/item/disc-magnets/small-samarium-cobalt-disc-magnets/26dre1613?. [Accessed 21 May 2012].

[11] D. Meeker, "Finite Element Method Magnetics: Version 4.2 User's Manual," 16 October 2010. [Online]. Available: http://www.femm.info/Archives/doc/manual42.pdf. [Accessed 23 May 2012].

[12] Y. Raitses, A. Smirnov and N. Fisch, "Cylindrical Hall Thrusters," in *AIAA Plasmadynamics and Lasers Conference*, San Francisco, CA, 2006.

[13] D. Knapp, Interviewee, *Interview with David Knapp.* [Interview]. 7 March 2012.

[14] K. A. Polzin, Y. Raitses, J. C. Gayoso and N. J. Fisch, "Comparison in Performance of Electromagnet and Permanent-Magnet Cylindrical Hall-Effect Thrusters," Princeton Plasma Physics Laboratory, Princeton, NJ, 2010.

[15] ASM International, "Chapter 2: Thermal Expansion," in *ASM Ready Reference: Thermal Properties of Metals*, Materials Park, OH, ASM International, pp. 9-16.

[16] MetalPrices.com, 6 May 2011. [Online]. Available: http://www.metalprices.com/historical/database/. [Accessed 22 May 2012].

[17] A. Smirnov, Y. Raitses and N. J. Fisch, "Electron Cross Field Transport in a Low Power Cylindrical Hall Thruster," *American Institute of Physics,* vol. 11, no. 11, pp. 4922-4933, 2004.

[18] A. Smirnov, Y. Raitses and N. J. Fisch, "Enhanced Ionization In the Cylindrical Hall Thruster," *American Institute of Physics,* vol. 8, no. 2, pp. 852-857, 2003.

[19] Y. Raitses and N. J. Fisch, "Parametric Investigations of a Nonconventional Hall Thruster," *American Institute of Physics,* vol. 8, no. 5, pp. 2579-2586, 2001.

[20] J. Kurzyna and D. Danilko, "IPPLM Hall Effect Thruster - Design Guidelines and Prelimninary Tests," in *International Electric Propulsion Conference, IPEC,* Wiesbaden, Germany, 2011.